

# Lateral Resistance of Unreinforced Masonry Walls Strengthened With Engineered Cementitious Composite

Hyun-Ki Choi<sup>1</sup> · Baek-II Bae<sup>2</sup> · Chang-Sik Choi<sup>3</sup>

Received: 14 June 2015 / Revised: 21 September 2015 / Accepted: 11 October 2015 / Published online: 1 June 2016  
© Iran University of Science and Technology 2016

**Abstract** Replacement of existing unreinforced masonry (URM) walls, commonly used as a non-structural member in apartments, with new reinforced concrete (RC) components has been used as a reliable method when remodeling is carried out. However, special care needs to be taken when URM walls are removed not to waste construction time and materials. Therefore, retrofitting existing URM walls can be deemed a better solution rather than replacing URM walls with RC ones. Using shotcrete is one of retrofitting techniques of URM walls. However, using normal shotcrete cannot improve adequate ductility and may cause brittle failure at a wall frame or slab connection. Therefore, new materials, such as engineered cementitious composite (ECC) and ultra-high performance concrete (UHPC) have emerged to resolve the problem of normal shotcrete by increasing ductility and toughness of retrofitting materials. In this study, sprayed ECC was used to increase both strength and ductility of existing URM walls. The results of two retrofitted URM walls under lateral quasi-static loading were compared to non-retrofitted one. One strengthened wall, retrofitted masonry wall (RTM)-ECC, was just sprayed and anchored to

a wall base. Another strengthened wall, RTM-ECC-WM, was the same as RTM-ECC except for addition of wire mesh. The retrofitted specimens showed significant increase of strength, ductility, and energy dissipation capacity in comparison with the control one. In addition, RTM-ECC-WM indicated higher strength degradation due to the load transferring effect of wire mesh than RTM-ECC.

**Keywords** Unreinforced masonry (URM) · Wall · Sprayable engineered cementitious composite (ECC) · Strength enhancement

## 1 Introduction

Remodeling is sometimes more effective and efficient than new construction in terms of time and economy. Combining generations of an apartment is one of attractive remodeling methods to widen areas of generations. For instance, obtaining a wider one generation apartment is available via combination of two normal generations without building a new structural member. This type of remodeling can be performed by making new openings on existing walls or removing those walls [1].

In particular, masonry walls parallel to a long side of a plan were used for many old row houses to separate generations. Removing those partition walls rarely affects seismic capacity of structures. However, new reinforced concrete (RC) walls are preferred to improve seismic capacity of such old structures which do not meet the current code requirements and to use existing spaces more efficiently when remodeling is carried out. However, constructing new RC walls in existing structures is difficult and not efficient from the standpoint of time and cost. This, as a result, can cause serious impediments to an effective remodeling.

✉ Hyun-Ki Choi  
chk7796@kyungnam.ac.kr

Baek-II Bae  
reise101@hanyang.ac.kr

<sup>1</sup> Department of Fire and Disaster Prevention Engineering, Kyungnam University, Changwon, Gyeongsangnam-Do 631-701, Republic of Korea

<sup>2</sup> Research Institute of Industrial Science, Hanyang University, 17 Haengdang-Dong Seongdong-Gu, Seoul 133-791, Republic of Korea

<sup>3</sup> Department of Architectural Engineering, Hanyang University, 17 Haengdang-Dong Seongdong-Gu, Seoul 133-791, Republic of Korea

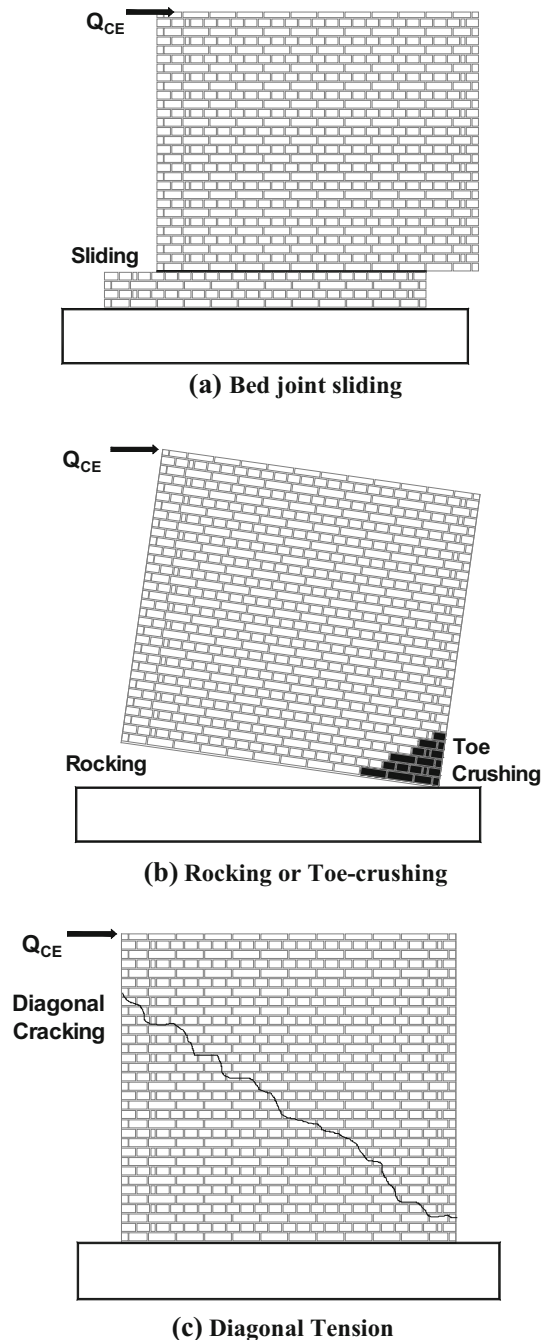


**Fig. 1** Types of failure modes for unreinforced masonry walls

Therefore, strengthening existing structural members is recommended to reduce the amount of existing members and removed and simultaneously avoid new construction. In this case, both time and cost needed for removal can be saved and walls with large flexural stiffness can be used as members for resistance of lateral loading by strengthening unreinforced masonry (URM) walls used as partition walls.

This research was conducted to investigate the effect of a strengthening technique using sprayable engineered

cementitious composite (ECC) on URM walls since simple and fast construction can be achieved using sprayable ECC [2, 3]. For this purpose, experimental tests were carried out using specimens designed and constructed in the pattern of an old row house.

## 2 Literature Review

Many types of retrofitting method for masonry were tested and analyzed. ElGawady et al. [4–6] carried out experimental studies on strengthening URM walls. ElGawady [4] summarized numerous conventional techniques, such as shotcrete, grout injection and external reinforcement. The disadvantages of these techniques are long construction time, reduced available space in building, distorted esthetics of the existing wall and increase in the mass of building. To solve these types of problem, ElGawady et al. [5] proposed and studied other retrofitting material, such as fiber reinforced plastic (FRP). Although FRP showed good performance in strength enhancement, it showed several critical problems, such as anchorage failure, limited energy dissipation and brittle mode of failure.

ElGawady [6] and Jabarov et al. [7] suggested a strengthening method for damaged URM walls using shotcrete (steel rebar and mortar). Shotcrete overlays are sprayed onto the surface of a masonry wall over a wire mesh. It is very convenient method in construction compared with conventional techniques and less costly than in situ jacket retrofitting method. Basically, shotcrete layer thickness is dependent on the seismic demand and it can be determined considering overlay as reinforced concrete shear wall. In general, the overlay thickness is at least 60 mm. The shotcrete overlay is typically reinforced with a minimum steel reinforcement ratio of shear wall in the shape of wire mesh to control crack. Retrofitting using shotcrete significantly increases the ultimate capacity of the retrofitted walls. In the diagonal tension test, shotcrete layer significantly increase the capacity of retrofitted wall. Although in diagonal tension test, the improvement in the cracking load was very high, and in a static cyclic test, the increment in the cracking load was insignificant. Other problem of applying shotcrete layer is quantification. There is no exact rule for retrofitting area or thickness. It is only constructed according to the construction availability and referring to the shear wall design.

According to most of test results, load-carrying capacity of URM walls considerably improved. However, it was found that ductility requirements were not properly satisfied since most of the strengthening materials had brittle material properties.

Fig. 2 Retrofitting concept

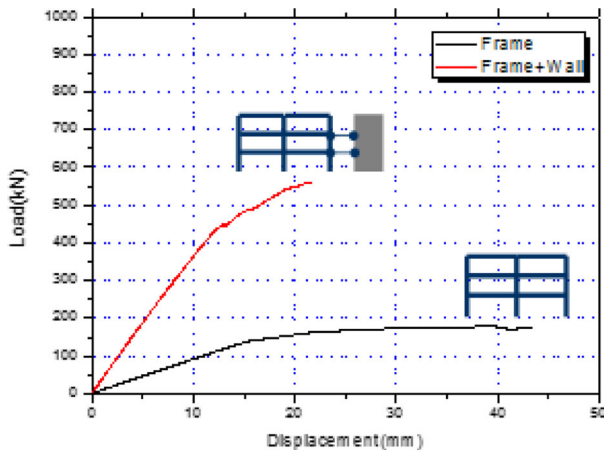
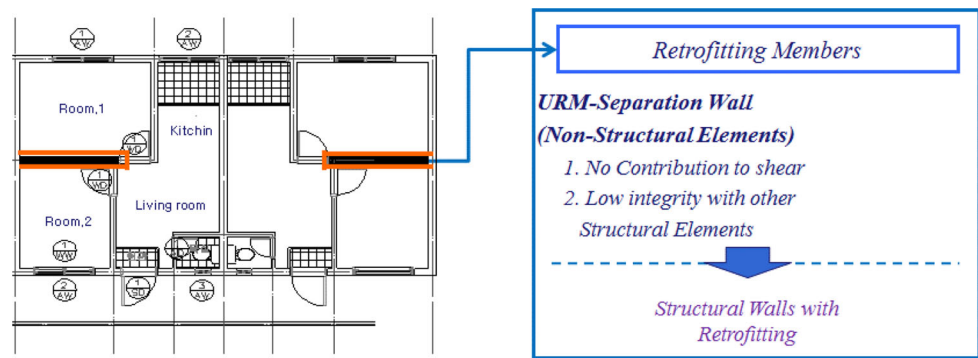


Fig. 3 Push-over analysis results of frames with and without wall

### 3 Performance Assessment of URM and Strengthened Walls

In case of row houses, there is large difference between long and short sides in terms of masonry amount, which can induce unbalanced failure of an entire structure. Moreover, a strengthening technique needs to improve not only load-carrying capacity but also ductility.

In general, URM walls do not or hardly have lateral force resistance. However, an aimed strengthening level was determined through predicting lateral resistance of URM walls using the estimation equation suggested by FEMA 356 for in-plane resistance under lateral force. Based on existing research results, FEMA 356 suggests guides for design of URM walls to resist lateral force and evaluation of existing structures [1]. Moreover, it presents how to assess structures with damage or loss of capacity for strengthening.

#### 3.1 Strength of URM Walls

Resistance of URM walls can be predicted using shear strength estimation equations suggested by FEMA 356. Shear strength of URM can be determined by bed joint sliding, lifting, compression failure of masonry, or diagonal

tension failure as follows; and these types of failure of unreinforced masonry walls were depicted in Fig. 1.

$$Q_{CE} = V_{bjs} = v_m A_n \tag{1}$$

$$Q_{CE} = V_r = 0.9 \alpha P_E \left( \frac{L}{h_{eff}} \right) \tag{2}$$

$$Q_{CE} = V_{tc} = \alpha P_E \left( \frac{L}{h_{eff}} \right) \left( 1 - \frac{f_a}{0.7 f'_m} \right) \tag{3}$$

$$Q_{CE} = V_{dt} = f_{dt} A_n \left( \frac{L}{h_{eff}} \right) \left( 1 + \frac{f_a}{f_{dt}} \right) \tag{4}$$

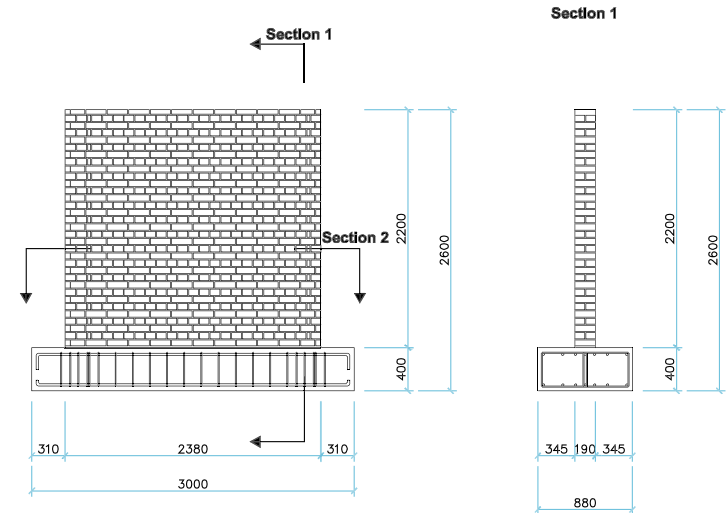
where  $Q_{CE}$  is the expected lateral strength of URM walls,  $V_{bjs}$  is the lateral resistance under bed joint sliding failure,  $V_r$  is the strength of wall or pier based on be rocking failure,  $V_{tc}$  is the strength based on compressive stress for wall,  $V_{dt}$  is the strength based on diagonal tension stress for wall,  $A_n$  is the mortar bonding area;  $h_{eff}$  is the wall height;  $L$  is the wall length;  $P_E$  is the estimated axial pressure on a wall;  $v_m$  is the sliding shear strength of a bed joint;  $f'_m$  is the compressive strength of masonry;  $f_{dt}$  is the diagonal tension stress;  $\alpha$  is the boundary condition constant; and  $f_a$  is the axial compressive stress.

#### 3.2 Determination of Strengthening Level

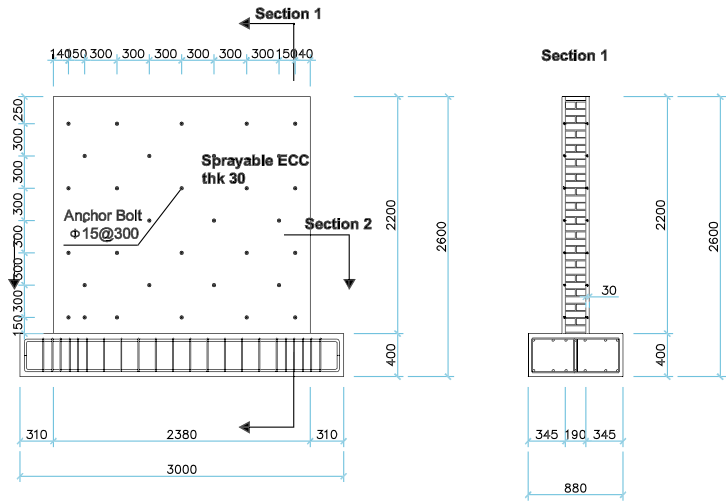
Currently, there is no reliable method to precisely compute a strengthening level of URM walls strengthened with sprayable ECC. In addition, there are limited experimental and analytical research results with regard to the strengthening technique using sprayable ECC. Meanwhile, in case of URM walls retrofitted with shotcrete similar to sprayable ECC, shear strength increased up to three times in comparison with that of URM walls. However, it was concluded that improving ductility was not effective when shotcrete was used as a strengthening material [4–7]. Abrams and Lynch [8] examined the specimens strengthened with shotcrete and FRP composites. They reported that the method for computing strength of RC walls could be used for predicting that of walls retrofitted with shotcrete.

Experimental tests were carried out to investigate structural behavior of URM walls strengthened with

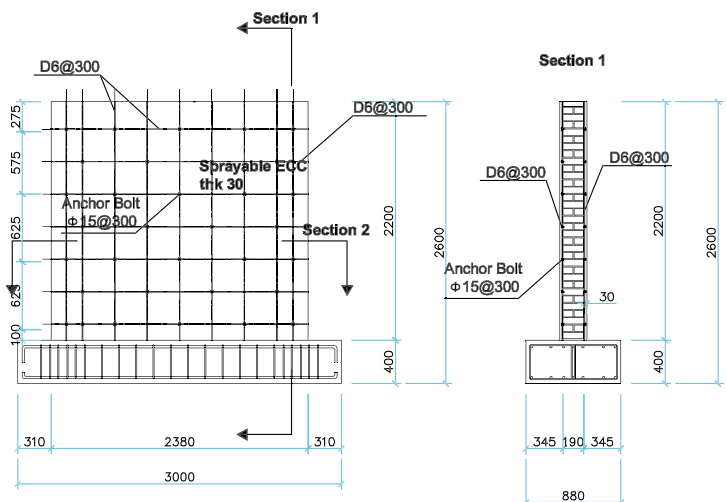
**Fig. 4** Specimen reinforcement details, unit (mm)



(a) URM-0.92



(b) RTM-ECC



(c) RTM-ECC-WM

different materials. The specimens were designed and constructed based on the real three-story rahmen-type row house built in the 1970s. Figure 2 depicts the plan and details of the three-story row house.

To determine a proper strengthening amount, the base shear of two spans of the three-story row house was analyzed using OPENSEES [9, 10]. The row house was modeled with models provided in OPENSEES. Beams and columns were modeled with fiber elements and joints were modeled with beam-column joint elements. To model the bar slip behavior at joint area, we also use pinching 4 model. The row house indicated load-carrying capacity of 190 kN based on the push-over analysis result. According to Korea Building Code (KBC-S-09) [11] and International Building Code [12], the resistance of the row house should be 475 kN if a response spectrum value of 3 for an ordinary moment frame is applied. In this study, the strengthening level was, therefore, decided to closely meet the requirement of KBC-S-09. In other words, the aimed strengthening level was 285 kN (475 ~ 190 kN) for a two span case. According to the push-over analysis on the two-span moment frame and the frame plus URM walls as seen in Fig. 3, a moment frame can show appropriate lateral resistance without plan modification if URM walls are strengthened using 30 mm sprayable ECC for both sides [13, 14].

To specify the retrofitting layer thickness, we referred to the literature that Sprayable ECC was used as retrofitting material for perforated reinforced concrete shear wall which was performed by Choi [15]. The results show that the evaluated effective shear strength was equivalent to direct tensile strength of ECC. Using this value in reinforced concrete shear strength equation proposed by ACI [16] or other researchers, retrofitting layer of 30 mm thick was adopted on both sides of the masonry wall to withstand the present seismic demand proposed in KBC-S-2009 [11].

## 4 Specimen Plan and Test Method

Specimens were fabricated and tested under quasi-static cyclic loading to appraise the strengthening technique suggested for URM walls in this study. The following specimens were constructed:

- URM-0.92: URM wall served as the control specimen
- RTM-ECC: URM wall strengthened with sprayable ECC and anchor bolts were used to avoid overturning
- RTM-ECC-WM: URM wall retrofitted with sprayable ECC and anchor bolts were connected with wire mesh.

### 4.1 Specimen Plan

The control specimen (URM-0.92) was based on the URM partition walls of the row house in the 1970s. As provided in Fig. 4 and Table 1, masonry walls for both controlled and strengthened specimens were mainly constructed with cement bricks and ordinary mortar using 1:1 full scale ratio. The aspect ratio of the specimens was 0.92 which is the same as the URM partition walls of the three-story row house.

The specimens were built on the precast base. When it comes to strengthening technique, two URM walls were strengthened with only sprayable ECC and sprayable ECC plus wire mesh, respectively.

### 4.2 Sprayable ECC

The concept of the sprayable ECC technique by Kim [2] was adopted in this study. Commercially available ECC and polyvinyl alcohol (PVA) fiber were used [Fiber volume fraction 2 %; (PE-short fiber; 1.5 %) + 0.5 (PP-long fiber; 0.5 %)]. Sprayable ECC has better bond capacity than ordinary ECC and the same tensile strength and deformability as ordinary ECC even after it is sprayed (refer to Fig. 5).

Figure 6 depicts the stress–strain response of sprayable ECC. The response was obtained through tensile testing in the laboratory. As seen in Fig. 6, after cracks had occurred, strain hardening was observed and ultimate strain reached 0.018. Moreover, the tensile strength of the concrete was 4.2 MPa which was 1.8 times ordinary concrete. Due to this material property, sprayable ECC was expected to improve deformability of URM walls unlike ordinary shotcrete.

**Table 1** Properties of test specimens

Specimen	$H$ (mm)	$L$ (mm)	Aspect ratio	$t_{\text{URM}}$ (mm)	$t_{\text{ECC}}$ (mm)	Wire mesh spacing (mm)	Shear dowel spacing (mm)	Brick element (mm)
URM-0.92	2380	2400	0.92	190	–	–	–	190 × 90 × 57
RTM-ECC					30 (one side)	–	600	
RTM-ECC-WM					30 (one side)	300	600	

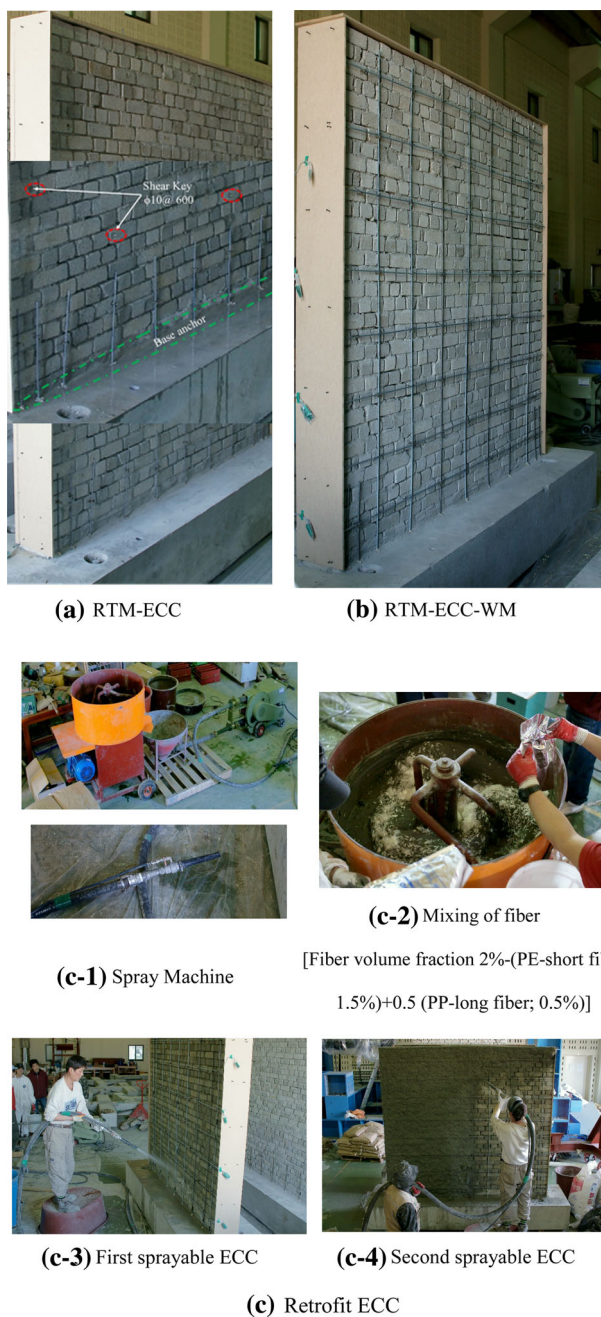


Fig. 5 Procedure of retrofit

### 4.3 Brick, Mortar and Wire Mesh

Commercially available cement bricks with dimensions of  $190 \times 90 \times 57$  mm were used to meet a 1:1 full scale ratio in comparison with the three-story row house-(refer to Fig. 2). Bed joints with 10 mm thickness, were used. Average compressive strength of the bricks was obtained as 15.7 MPa. Also, commercially available mortar was applied and average compressive strength of the mortar was measured as 8.4 MPa using specimens with dimensions of  $50 \times 50 \times 50$  mm.

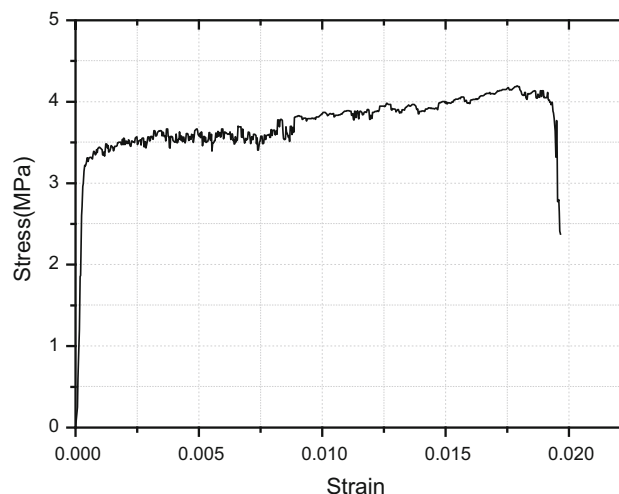


Fig. 6 Stress-strain relation in tension of sprayable ECC

It was reported that strengthening materials on the surface of RC walls were detached to the out-of-plane direction under large loading [11]. To avoid this failure, shear keys with 10 mm diameter were vertically constructed to the wall surface before sprayable ECC was applied. The shear keys were used for both strengthened specimens and had a space of 600 mm which was two times that of the wire mesh to fix the wire mesh (refer to Fig. 5).

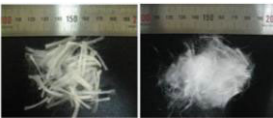
The wire mesh was used to enhance bond capacity of sprayable ECC and to play a role of controlling cracks as steel reinforcement. The wire mesh was placed with a space of 300 mm. One layer of the wire mesh was applied only for each side of RTM-ECC-WM. The wire mesh consisted of high tension steel with a yield strength of 745 MPa and a tensile strength of 800 MPa- (refer to Table 2).

### 4.4 Test setup and loading protocol

The test setup is illustrated in Fig. 7. As stated earlier, the specimens were constructed on the precast RC base tied to the strong frame in the laboratory. Small compressive force was applied through self-weight of the URM wall and the steel loading beam since the URM wall was a non-structural member. Lateral force was generated using a 1000 kN actuator attached to the steel loading beam on the top of the URM wall specimen. Furthermore, the out-of-plane support frame was set up to prevent the URM wall from out-of-plane buckling as seen in Fig. 7.

The specimens were examined under displacement control. Loading protocol is shown in Fig. 8. The displacement control was based on the rotational angle of the specimens. In other words, a drift ratio of distance from the specimen bottom to the center of the actuator to lateral displacement increased from 0.1 % with an increment of

**Table 2** Characteristics of materials

Chemical properties of ECC powder									
	Density (g/mm <sup>3</sup> )	SiO <sub>2</sub>	Al <sub>2</sub> O <sub>3</sub>	Fe <sub>2</sub> O <sub>3</sub>	CaO	MgO	SO <sub>3</sub>		
OPC	3.15	22.75	5.93	3.37	61.73	2.53	1.97		
Silica powder	2.66	95.5	1.95	–	–	–	–		
Silica sand	2.64	969	1.44	0.34	0.11	0.03			
Properties of fiber									
Ingredient	Density (g/mm <sup>3</sup> )	Length (mm)	Diameter (μm)	Surface treatment	Melting point (°C)	Thermal decomposition (°C)	Tensile strength (MPa)	Young's modulus (GPa)	Elongation (%)
PVA	1.3	6–8	39	Oiling agent	170	263	1700	29.4	3–113
									
(PE+PP)									
Mix proportion									
W/C	Fiber volume fraction [%]		Unit weight (kg/m <sup>3</sup> )			Admixture			
	PE (Polyvinyl alcohol)-short fiber	PP (polyethylene)-long fiber	cement	water	sand				
0.45	1.5	0.5	1041.47	416.59	468.66	Viscosity agent, Superplasticizer, thickening agent			
Mechanical properties of specimen									
Brick (Mortar; cement: sand = 1:1)			Sprayable ECC						
Compressive strength of brick element (MPa)		Compressive strength of mortar (MPa)	Compressive strength of ECC (MPa)		Tensile strength of ECC (MPa)		Tensile strain of ECC (MPa)		
15.7		8.4	41		4.18		0.018		
Anchor bolt (shear key) φ10@600		Yield Strength of Wire mesh (MPa)		Wire mesh D6		Tensile strength of wire mesh (MPa)			
		745				800			

0.1 (i.e., 0.1, 0.2, 0.3, 0.4, and 0.5 %). Positive and negative cyclic loading was repeated three times per drift ratio. Load and main displacement were measured with actuator mounted load cell and linear variable differential transformer (LVDT), respectively.

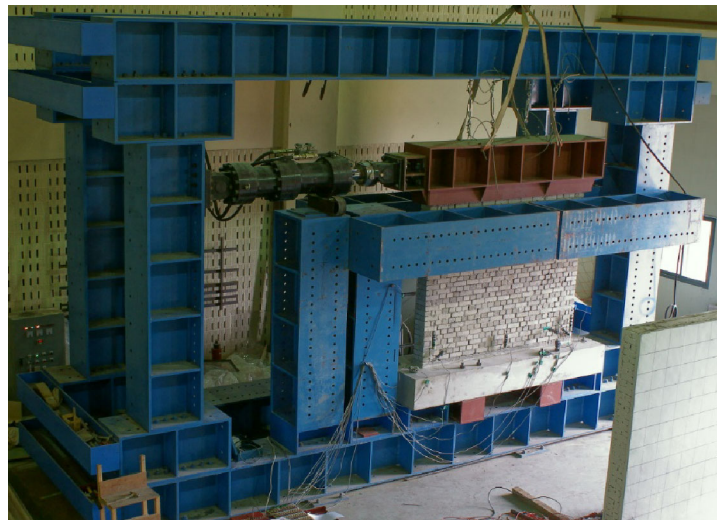
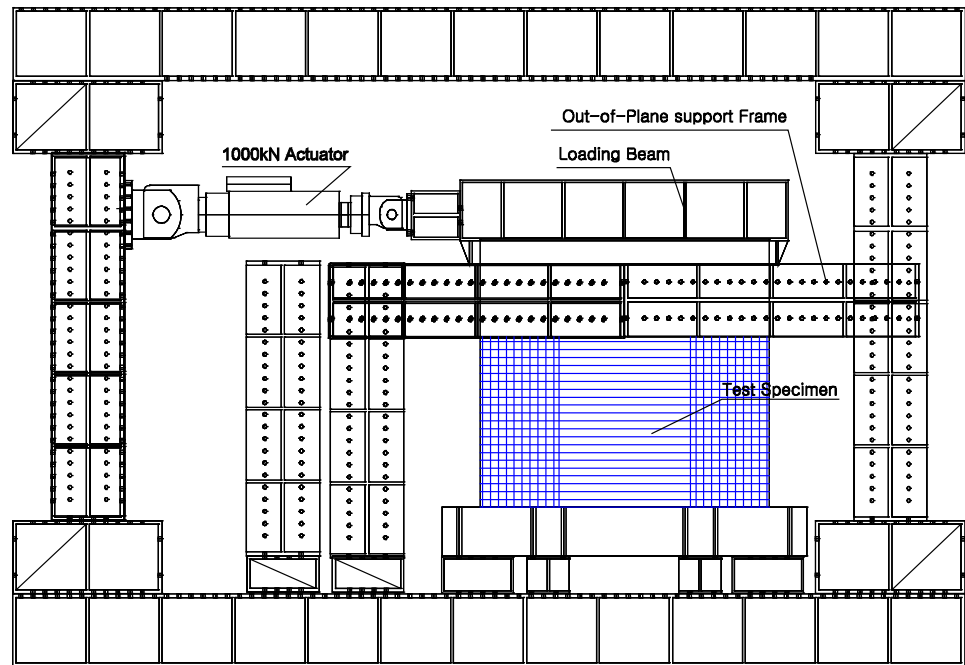
## 5 Test results

### 5.1 Crack Pattern and Failure Mode

Crack patterns and failure modes of the specimens are shown in Fig. 9. A detailed description of the specimens is as follows.

URM-0.92: this was the non-strengthened specimen. An initial crack formed at the mortar of the URM wall bottom part at a positive drift ratio of 0.1 %. When a negative drift ratio reached 0.1 %, cracks were observed at the mortar between the base and the end of URM-0.92 as depicted in Fig. 9. As both positive and negative ratios reached 0.2 %, the initial cracks propagated towards the center of the wall following the mortar. The cracks kept propagating towards the center to 600 and 1200 mm and there was no visible damage at the other areas at a drift ratio of 0.3 and 0.4 %, respectively. At the 0.6 % drift ratio, the wall over the existing crack slipped and then the cement brick at the end side of the wall was crushed, resulting in failure of the wall specimen.

Fig. 7 Test setup



RTM-ECC: as stated before, this specimen was strengthened with sprayable ECC, both bottom and out-of-plane anchors. When a drift ratio reached 0.1 %, a hairline flexural crack was initiated at the region 200 mm apart from the bottom of the wall. The same behavior was observed at a drift ratio of  $-0.1$  %. The initial crack and shrinkage cracks widened as a drift ratio reached 0.2 %. A little slip of the wall occurred due to widening of the cracks at the end of the wall at the  $-0.2$  % drift ratio. As load increased, the cracks at both end sides of the wall propagated due to the wall lifting. When a drift ratio reached 0.3 %, the existing cracks propagated and widened more due to the wall lifting. At the 0.5 % drift ratio, compressive cracks on the brick at the end of the wall formed. Part of

sprayed ECC at the end side of the wall was detached due to compressive force at the 0.6 % drift ratio. When a drift ratio reached 0.9 %, ECC on the front side of the wall was locally crushed. Finally, RTM-ECC failed due to crushing of the brick at the 1.2 % drift ratio.

RTM-ECC-WM: sprayable ECC, bottom anchors, and wire mesh were used to strengthen this specimen. At the 0.1 % drift ratio, an initial crack formed at the wall end and shrinkage cracks propagated. The same crack pattern was observed at a drift ratio of  $-0.1$  %. After the 0.2 % drift ratio, existing cracks propagated and widened towards the center of the wall and new cracks formed between the wall and base. At the 0.4 % drift ratio, the cracks between the wall and base widened, and then part of steel rebar was



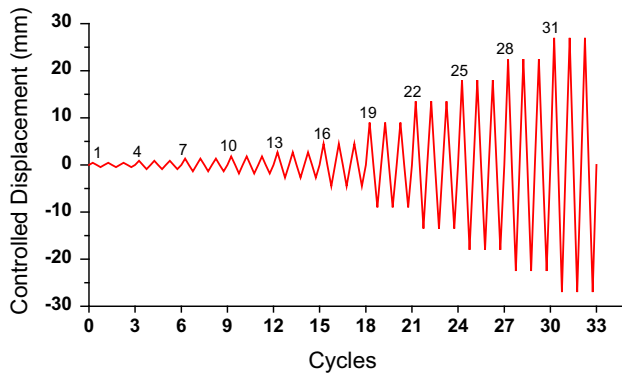


**Fig. 8** Loading protocol

pulled out. As load increased, the existing cracks did not propagate much, and at the 0.8 % drift ratio, the cracks were observed on the brick at the end of the specimen. When a drift ratio reached 1.3 %, the brick at the end of the wall was crushed and debonded at the interface between ECC and the wall occurred. RTM-ECC-WM failed due to crushing of both the brick at the end of the wall and ECC at the 1.5 % drift ratio.

## 5.2 Load–Displacement Response

Load–displacement responses of the three specimens are depicted in Fig. 10. Detailed results of each specimen are as follows.

URM-0.92: After the initial cracks occurred, no additional load was transferred between the wall and base due to the cracks on the mortar between the wall and base, resulting in the ultimate load of 23 kN at the 0.2 % drift ratio. After a drift ratio of 0.5 %, displacement kept increasing without load increase due to the wall slip after the cracks on the mortar between the wall and base. Therefore, the failure was considered to occur due to the wall lifting at the 0.4 % drift ratio after the ultimate load.

RTM-ECC: The ultimate load was measured as 74 kN at a drift ratio of 0.25 %. However, after reaching the peak load value, the specimen retained an acceptable load-carrying capacity, and consequently reached a lateral displacement of 1.3 %. At the 0.6 % drift ratio, initial debonding at ECC occurred, and then crushing of ECC was observed at the bottom part of the wall at a drift ratio of 0.9 %. Finally, RTM-ECC failed due to the crushing of the bricks when a drift reached 1.2 %. Compared to the control specimen (URM-0.92), structural performance of RTM-ECC improved in terms of both strength and deformability since steel rebar at the bottom prevented the specimen from slipping. Due to the larger stiffness of the specimen than that expected, the failure of the specimen was induced by the anchor pulling out prior to failure of the wall itself. As a

result, the effect of deformation hardening of the specimen was not significant.

RTM-ECC-WM: When it comes to initial stiffness and load pattern, RTM-ECC-WM showed a similar behavior to RTM-ECC. However, in case of RTM-ECC-WM, pulling out stress in the base was spread out to the entire wall since strain in steel reinforcement was distributed to the entire wall. Although stiffness was reduced at the 0.2 % drift ratio, larger maximum load-carrying capacity of 98 kN was obtained at a drift ratio of 0.4 % than RTM-ECC. Furthermore, after the peak load value, there was no sudden load dropping in comparison with RTM-ECC. This was attributed to the stress distribution in the entire wall. However, as with RTM-ECC, shear deformability of RTM-ECC-WM was not remarkable due to the largely improved stiffness.

From both strengthened specimens, much larger initial stiffness values were obtained than that of the control specimen as shown in Fig. 10d. This was attributed to the enhanced integrity of URM walls due to ECC strengthening.

## 6 Evaluation of Strengthening Effect

### 6.1 Effect in Terms of Strength and Ductility

The main test results of the three specimens are summarized in Table 3. Yield and maximum strengths as well as corresponding displacements are provided for positive and negative loading. As listed in Table 3, strength of RTM-ECC and RTM-ECC-WM increased by 3.2 and 4.3 times that of URM-0.92. This strength improvement was more than three times that obtained using shotcrete by ElGawady et al. [6]. This notable performance was probably due to the large tensile strength and ductile failure mode of ECC under compression.

Ductility at ultimate and failure was defined to be the ratio of displacement at ultimate and failure to displacement at yielding, respectively. Even though large displacement of URM-0.92 was recorded due to the rotation caused by the wall lifting after the peak load, ductility of the strengthened specimens was similar or even better in comparison with URM-0.92. As mentioned, continuous load resistance was observed from RTM-ECC. In case of RTM-ECC-WM, strength was smoothly decreased after the ultimate load, and thus large deformation was obtained. Ductility values of RTM-ECC and RTM-ECC-WM increased 1.2 and 1.25 times more than that of URM-0.92, respectively. This improvement was mainly due to the rotational resistance of the wall by steel rebar which was between the wall and base as well as spread crack formation by flexure of ECC.

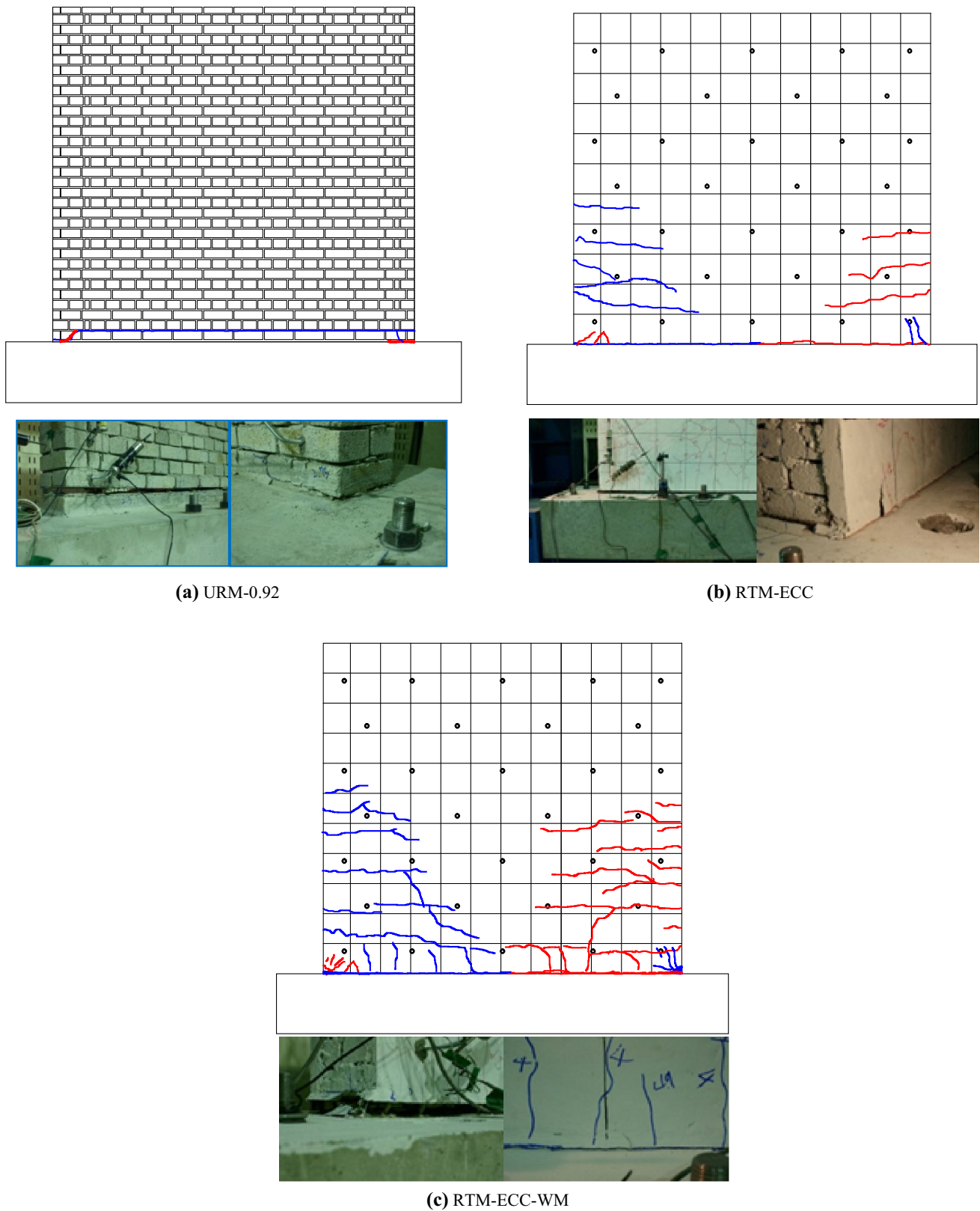


**Fig. 9** Crack formation and failure mode of specimens

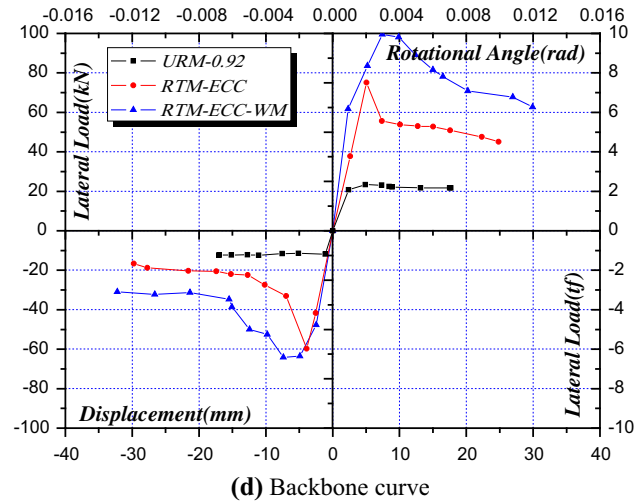
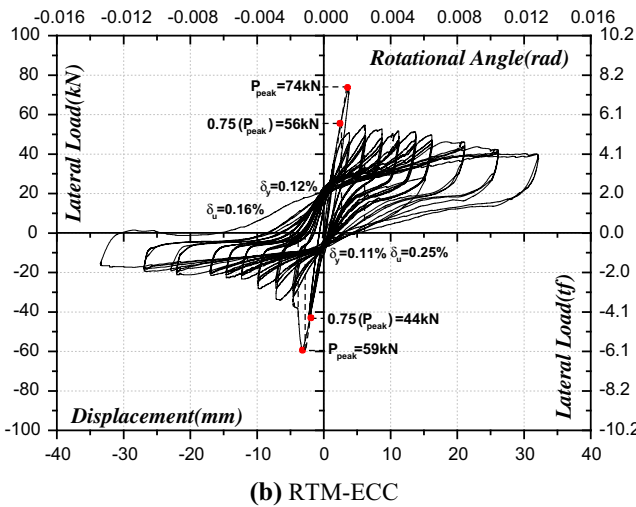
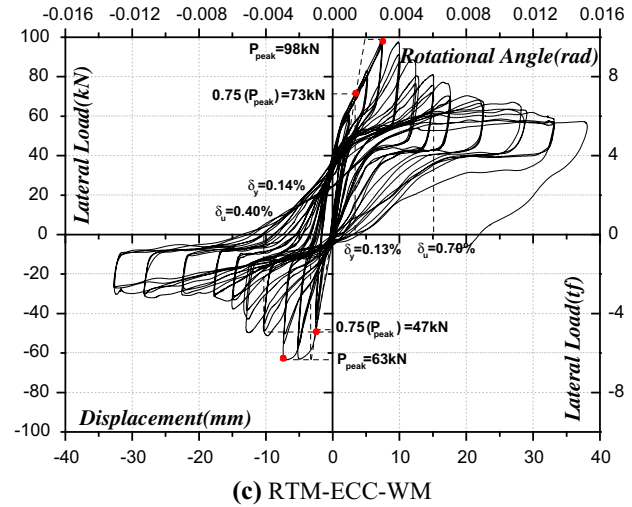
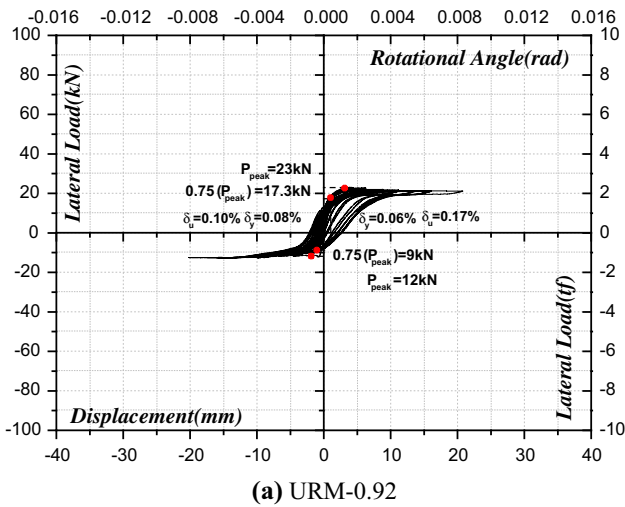


Fig. 10 Load-displacement relationships of specimens

### 6.2 Deformation of Specimens

The resistance of the tested specimens expressed as Eq. (5) as suggested by Abrams and Lynch [8] for URM specimens strengthened with shotcrete, was adopted for the study. Comparison with the test results are provided in Table 3.

$$V_{\text{shot}} = 0.27 \sqrt{f'_c} h d \quad (5)$$

where  $f'_c$  = compressive strength of concrete (MPa),  $h$  = wall thickness (mm) and  $d$  = wall length (mm). There is remarkable difference between the test results of strengthened specimens and the theoretical ones by Eq. (5) as listed in Table 3 [17]. This is probably because Eq. (5) applies when the specimens failed due to big diagonal tension cracks in the strengthened face with shotcrete. However, in case of the specimens strengthened with ECC,

failure was mainly induced by pulling out of the anchor since the specimens with ECC had considerable resistance against diagonal tension cracks.

When the specimens were constructed, wired strain gages (WSGs) were attached on anchor steel rebars. The strain data obtained was used to analyze anchor failure in detail. Strain distributions, measured from the location of 100 mm from the bottom of RTM-ECC and RTM-ECC-WM, are depicted in Figs. 11 and 12, respectively. It is expected for the specimens to be subjected to the largest tensile force at the location of 140 mm from the loading point. Therefore, the strains of each specimen at the location were compared to each other. The strains of RTM-ECC-WM were larger than those of RTM-ECC as shown in Figs. 11 and 12. In other words, after RTM-ECC underwent anchor failure at a drift ratio of 0.2 %, the strains of RTM-ECC did not increase much, even though a drift ratio

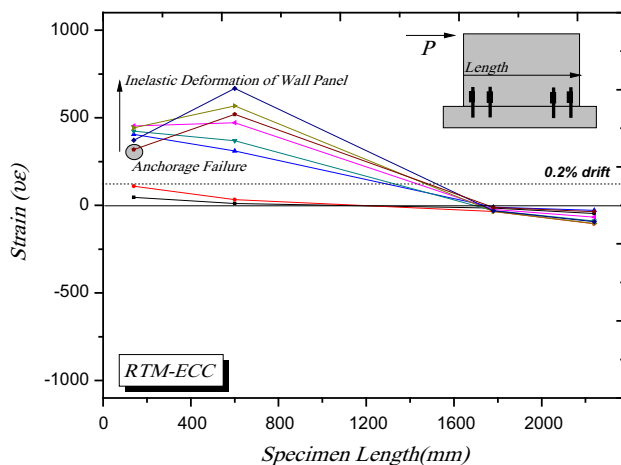
**Table 3** Summary of test results

Specimens	$P_{cr}$ (kN)	$P_y$ (kN)	$P_{max}$ (kN)	$\delta_y$ (mm)	$\delta_{max}$ (mm)	$\theta_y$ (%)	$\theta_{max}$ (%)	$\mu\left(\frac{\mu_{retrofit}}{\mu_{URM}}\right)$	$P_{calculation}$ (kN)	$\frac{P_{max}}{P_{calculation}}$	$\frac{P_{u,retrofit}}{P_{max,URM}}$
URM-0.92											
Pos	19	17	23	1.5	12.6	0.06	0.5	8.3 (1)	23	1	–
Neg	–10	–9	–12	–1.8	–9.8	–0.08	–0.4	5.4 (1)			–
RTM-ECC											
Pos	38	56	74	2.6	26.4	0.11	1.3	10.1 (1.21)	188	0.39	3.2
Neg	–22	–44	–59	–2.9	–26.9	–0.12	–1.1	9.2 (1.70)			4.8
RTM-ECC-WM											
Pos	44	73	98	3.39	33	0.13	1.34	10.3 (1.24)	216	0.45	4.3
Neg	–32	–47	–63	–3.4	–32	–0.14	–1.3	9.4 (1.74)			5.8

All estimates associated with moment and shear computed based on actual material properties

$P_{cr}$  initial crack load (measured),  $P_y$  yield load by Park's method (measured),  $P_{max}$  peak load (measured),  $\delta_y$  yield displacement (measured),  $\delta_{max}$  peak displacement (measured),  $\theta_y$  drift corresponding to the yielding,  $\theta_{max}$  drift corresponding to the yielding,  $u$  ductility ( $\delta_{max}/\delta_y =$  deformation capacity),  $P_{calculation}$  strength of masonry wall predicted by FEMA 356 and research results of Abrams

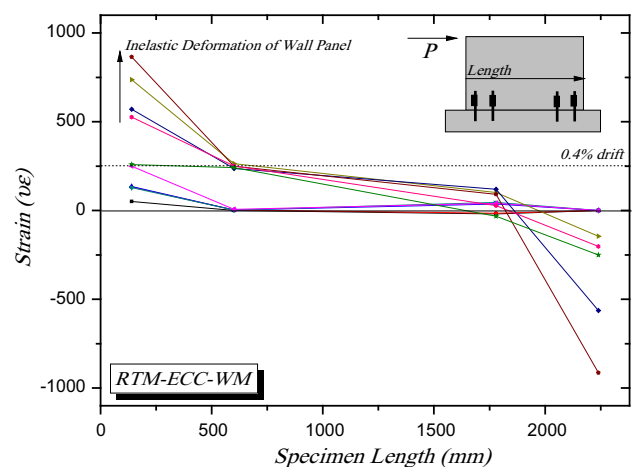
$$\left( V = V_m + V_c, \quad V_c = 0.27 \sqrt{f'_c} h d + \frac{N_u d}{4l_w} \right)$$

**Fig. 11** Strain distributions of specimen RTM-ECC

increased. However, in case of RTM-ECC-WM, the strains kept increasing even after anchor failure at the 0.4 % drift ratio, which means that the anchor continuously resisted the wall rotation. Anchor failure of each specimen resulted in slip and deformation of steel rebar, and thus inelastic behavior of each specimen.

### 6.3 Energy Dissipation Capacity

Energy dissipation capacity of the specimens depends on the frictional force between the wall and base, crack formation, crushing of brick, and the yielding and rupture of

**Fig. 12** Strain distributions of specimen RTM-ECC-WM

steel rebar. Energy dissipation capacities for each specimen are shown in Fig. 13. Both strengthened specimens presented much larger dissipation capacity than the control specimen. When URM-0.92 failed, RTM-ECC and RTM-ECC-WM indicated 4.7 and 21.4 times larger dissipation capacity than URM-0.92, respectively. When RTM-ECC failure occurred, energy dissipation capacity of RTM-ECC-WM was 4.5 times larger than that of RTM-ECC.

The high tension steel rebar used in this study was specially fabricated to have a smaller diameter than ordinary steel rebar for maximizing crack distribution effect of ECC and ensuring workability. It is difficult to expect large

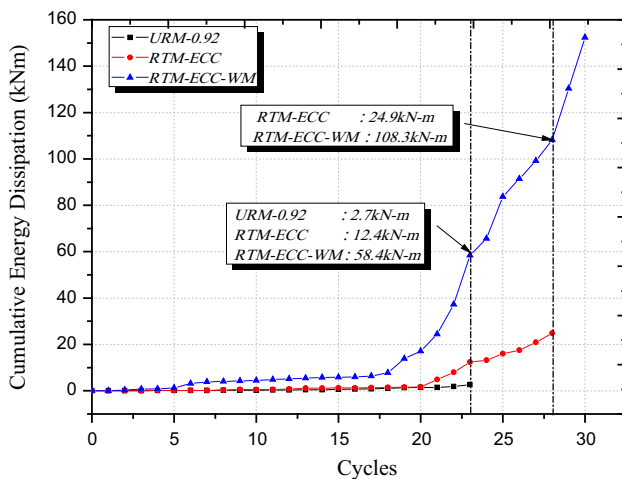


**Fig. 13** Energy dissipation capacity of specimens

deformation when such high tension steel rebar is under local stress. Due to this phenomenon, contribution of such high tension steel rebar to the energy dissipation capacity of RTM-ECC was not significant since the steel rebar in RTM-ECC was deformed mainly by stress at the connection part, and thus remained elastic during the test. On the contrary, stresses were distributed well to the steel rebar in RTM-ECC-WM through the wire mesh from the bottom and up to top of the wall. Thus, the steel rebar placed in the loading direction was properly deformed, resulting in a large energy dissipation capacity of RTM-ECC-WM.

## 7 Conclusions

In this study, tests were carried out to investigate structural performance of URM walls strengthened with sprayable ECC for improving seismic capacity. The following conclusions can be drawn:

1. Due to the high bond capacity of sprayable ECC, integrity of the URM specimen was improved. As a result, the specimens only strengthened with ECC whereas with both ECC and wire mesh indicated an initial stiffness of 1.8 and 3 times larger than that of the control specimen, respectively.
2. Both load-carrying capacity and ductility of the unstrengthened specimen increased through the strengthening technique using sprayable ECC. In case of RTM-ECC with 30 mm ECC on each wall side, strength and ductility were improved by 3.2 and 1.2 times more in comparison with URM-0.92, respectively. With both ECC and wire mesh, RTM-ECC-WM showed 4.3 and 1.25 times larger strength and ductility than URM-0.92, respectively.

3. In terms of strength, ductility, and stiffness, the effect of the wire mesh was not substantial. However, from the standpoint of energy dissipation capacity and crack formation, the wire mesh significantly contributed to structural performance of the wall through deformation increase of the wire mesh. Unlike conventional shotcrete, wire mesh can, therefore, help increasing energy dissipation capacity of structures strengthened with ductile materials, such as ECC.
4. While the stiffness increase of the wall contributed to the strength increase of the wall, it was the main reason of the anchor failure. Therefore, when the URM wall is strengthened, a special method is additionally needed to avoid such anchor failure due to lifting of the URM wall with increased stiffness. Moreover, further research is in need with regard to deformability assessment of a wall when the top and bottom parts of the wall are tied to each other.

**Acknowledgments** This research was supported by Basic Science Research Program through the National Research Foundation of Korea (No. NRF-2015R1D1A1A01059989, 15CTAP-C097470-01).

## References

1. Applied Technology Council ATC (2000) Prestandard and commentary for the seismic rehabilitation of buildings. FEMA-356, Federal Emergency Management Agency, Washington, DC, 7-1-22
2. Kim YY (2005) Development of a sprayable ductile fiber reinforced cementitious composite (ECC) based on micromechanics and rheological control. *J Korea Concr Inst (KCI)* 15(4):557–565
3. Victor CL, Dhanada KM, Antoine EN, James KW, James ML, Hwai CW, Yasou I (1994) On the shear behavior of engineered cementitious composites. *J Adv Cem Based Mater* 1(3):142–149
4. ElGawady M, Lestuzzi P, Badoux M (2004) A review of retrofitting of URM walls using composites. In: 4th International conference on advanced composite materials in bridges and structures
5. ElGawady M, Lestuzzi P, Badoux M (2006) Shear strength of URM walls retrofitted using FRP. *J Eng Struct* 28(12):1658–1670
6. ElGawady M, Lestuzzi P, Badoux M (2006) Retrofitting of masonry walls using shotcrete. In: Proceedings of NZSEE, paper-No. 45
7. Jabarov M, Kozharinov S, Lunyov A (1980) Strengthening of damaged masonry by reinforced mortar layers. In: 7th WCEE, Istanbul, vol 6, pp 73–80
8. Abrams DP, Lynch JM (2001) Flexural behavior of retrofitted masonry piers. In: KEERC-MAE joint seminar on risk mitigation for regions of moderate seismicity
9. McKenna F, Fenves GL (2000) The OpenSees Command Language Primer, PEER, University of California. <http://OpenSees.Berkeley.edu>
10. Lourenco PB (1996) Computational strategies for masonry structures. PhD thesis, Delft University, Netherlands, p 210
11. KBC-S-09 (2009) Korea building code requirements for structural concrete and commentary. Architectural Institute of Korea (AIK), Seoul, pp 335–360

12. International Code Council (2006) International Building Code, pp 373–383
13. Calvi G, Magenes G (1994) Experimental results on unreinforced masonry shear walls damaged and repaired. In: Proceedings of the 10th International brick masonry conference, vol 2(1), pp 509–518
14. Haider W, Dhanasekar M (2004) Experimental study of monotonically loaded wide spaced reinforced masonry shear walls. Aust J Struct Eng 5(2):101–118
15. Choi YC, Choi CS, Kim HM, Lee LH (2006) Shotcrete-retrofit of shear walls with an opening. J Korea Inst Struct Maint Insp 11(5):71–80
16. ACI 318 M-08 (2008) Building code requirements for structural concrete and commentary, vol 318. American Concrete Institute (ACI) Committee, Michigan, pp 299–334
17. Abrams DP (1997) Development of procedures to enhance the performance of rehabilitated URM buildings. NIST GCR 97-724-1, pp 2-1-48